



Experimental seismic testing of semi-reinforced stone masonry building in mud mortar

J. Bothara

Miyamoto International NZ Ltd., New Zealand

N. Ahmad

Earthquake Engineering Center, University of Engineering and Technology Peshawar, Pakistan

J. Ingham & D. Dizhur

Department of Civil and Environmental Engineering, The University of Auckland, Auckland.

ABSTRACT

The 2015 Gorkha earthquakes and associated aftershocks damaged or destroyed more than 30,000 school classrooms in Nepal. For future proofing, the Government of Nepal is constructing earthquake resilient school buildings using cement and steel in the areas accessible by motorable roads. However, transporting such construction materials to many of the inaccessible earthquake-affected areas is logistically challenging and financially nonviable, with stone and mud being the only construction materials that are readily available in such inaccessible areas.

Three multi-hazard resilient stone masonry school building typologies were developed that utilise abundantly available local materials. The conceptual design of these low strength masonry buildings is reported herein. Preliminary results are presented from an extensive experimental campaign that included shake table tests. Three prototype modular school buildings were designed with loadbearing walls composed of stone masonry in mud mortar and provided with light metal roof. The walls of the buildings incorporated horizontal bands and surface containment steel mesh on both surfaces of the walls. The containment mesh was tied with wires passing through the walls. Each prototype was constructed at 1/3rd and 2/3rd scale and was subjected to multiple base excitations with increasing amplitude up to 1.0g. The damage ranged from cracking to global/local sliding and rocking along the multiple bedding planes of the walls. The model buildings survived the intense shaking without triggering any unstable modes of failure, thereby confirming compliance of the proposed designs to applicable Nepal seismic standards.

1 INTRODUCTION

Unreinforced stone masonry buildings constructed in mud mortar were the most severely damaged building class (Dizhur, Dhakal, Bothara, & Ingham, 2015), (Bothara, Dhakal, Dizhur, & Ingham, 2016) in the M_w 7.8 2015 Gorkha earthquake which damaged or destroyed approximately 750,000 houses, 6,000 government buildings, and 30,000 school classrooms (NRA, 2016). As recommended by the post-earthquake reconstruction planning and ‘proofing’ against future earthquakes, the Government of Nepal (GoN) decided to reconstruct all schools as earthquake resilient.

In vehicular accessible areas, the Government of Nepal is constructing school buildings using ductile reinforced concrete (RC) frame type buildings, but transporting industrialised construction materials such as cement, structural steel and rebars is generally not feasible in the larger part of the inaccessible earthquake-affected areas, and the only construction materials that are economically available in abundance in such remote areas is stone and mud. The Government of Nepal hence commissioned a project to explore the suitability of using locally abundant materials for the construction of earthquake resilient school buildings.

To date, limited research is available on design and construction of earthquake resilient important facilities (such as schools) using stone masonry in mud mortar (Bothara, Ingham, & Dizhur, 2018). As part of the evidence-based design, an extensive experimental testing programme was undertaken to confirm compliance of school buildings constructed using locally available stone and mud materials to satisfy the Nepal Building Code. The testing programme included extensive basic tests on constituent materials, subassembly tests (prisms, wallettes and short piers) and shake table tests of three 1/3rd and another three 2/3rd reduced scale stone masonry model buildings. Discussed herein is the design concept of the proposed prototype school buildings and the basis of modelling and fabrication of the scaled models, along with the experimental procedures, observations and their interpretation as well as high-level test results.

2 DESIGN OF PROTOTYPE SCHOOL BUILDINGS

In the absence of established design standards for low strength masonry (LSM) buildings, the design concepts (Bothara, Ingham, & Dizhur, 2018) for earthquake resilience of the building was prepared based on available prescriptive guidelines (NBC, 1994), (IS, 1993), (Arya, Boen, & Ishiyama, 2013)), previous research (Jagadish, Raghunath, & Rao, 2002), (Navaratnarajah, Mayorca, & Meguro, 2012), (Navaratnarajah, Sakurai, & Meguro, 2009)) and observed and postulated failure modes of the LSM buildings and their consequences. As observed in past earthquakes, loss of integrity between masonry units and components of the building is one of the major threats against the survival of LSM buildings (Dizhur, Dhakal, Bothara, & Ingham, 2015), (Gautam & Chaulagain, 2016), (Bothara & Hiçyılmaz, 2008). Hence, the approach taken while developing earthquake resiliency of the proposed designs was to maintain integrity between the masonry units and building components and prevent any loss of building volume. Once the concept design was finalised, the structural design of the buildings was completed following classical mechanics and simplified engineering methods.

2.1 Damage Patterns of Low Strength Masonry Buildings

Local and global failure modes of LSM buildings when subjected to earthquake induced loading is inherent in the building morphology. The LSM buildings typically suffer from a lack of bonding between masonry units and masonry veneers, and effective connection between orthogonal walls and various building components, such as lack of wall to diaphragm connections. These deficiencies commonly lead to delamination and mechanism failure (expulsion of irregular stones) due to a lack of connection between outer veneers and irregular stones (Dizhur, Dhakal, Bothara, & Ingham, 2015), (Gautam & Chaulagain, 2016), (Bothara & Hiçyılmaz, 2008), and slumping or overturning of walls under face loading. Figure 1 presents photographs of failure examples, which includes local and global failure modes that are typically suffered by LSM buildings.



(a) Delamination and bulging of wall wythe, 2015 Gorkha earthquake, Nepal



(b) Out-of-plane collapse of wall led to collapse of roof and floor, 2015 Gorkha earthquake, Nepal



(c) Out of plane collapse of walls, destruction of top storey, 2015 Gorkha earthquake, Nepal



(d) Destruction of a village, during 2005 Kashmir earthquake, Pakistan



(e) In-plane wall and corner damage, 2005 Kashmir earthquake, Pakistan



(f) Roof collapse due to absence of wall-roof connections, 1999 Chamoli earthquake, India
(Photo credit: WHE, Report # 74)

Figure 1: Typical failure modes of stone masonry building with weak mortar

2.2 Design Proposals

Following the recommendations of the aforementioned guidelines as well as observed and postulated damage to low strength masonry buildings, the following four Design Types (DT) were developed that utilise the abundantly available local construction materials, with only minimal use of imported materials. The Design Types were one-storey high with a light metal roof and have the same architectural features and sizes. A sample drawing of the proposed two-room prototype is presented in Figure 2 and details of the proposed building types are as follows:

- **DT 1 (SM_RC):** Semi-dressed stone masonry in cement stabilised mud mortar with RC band, splints and containment mesh on wall surfaces,
- **DT 2 (SM_Gabion):** Semi-dressed stone masonry in mud mortar with galvanized iron gabion bands and containment mesh on wall surfaces
- **DT 3 (CSEB_RC):** Cement stabilized earth brick (CSEB) in cement stabilized mud mortar with RCC bands and vertical bars.
- **DT 4 (SM_Timber):** Semi-dressed stone masonry in mud mortar with timber bands and containment mesh on wall surfaces.

As noted above, the developed Design Types of stone buildings in mud mortar were provided with gabion, timber or reinforced concrete (RC) bands. To basket and thereby prevent disintegrity of the stone masonry walls, galvanized steel mesh was proposed on both surfaces of the walls, which were tied together by cross links (cross ties) passing through the walls.

The CSEB walls in cement stabilised mud mortar have been proposed for the areas where dressable stones are not available. Due to space limitations, the details presented here are limited to stone masonry buildings (DT 1, 2 and 4) only.

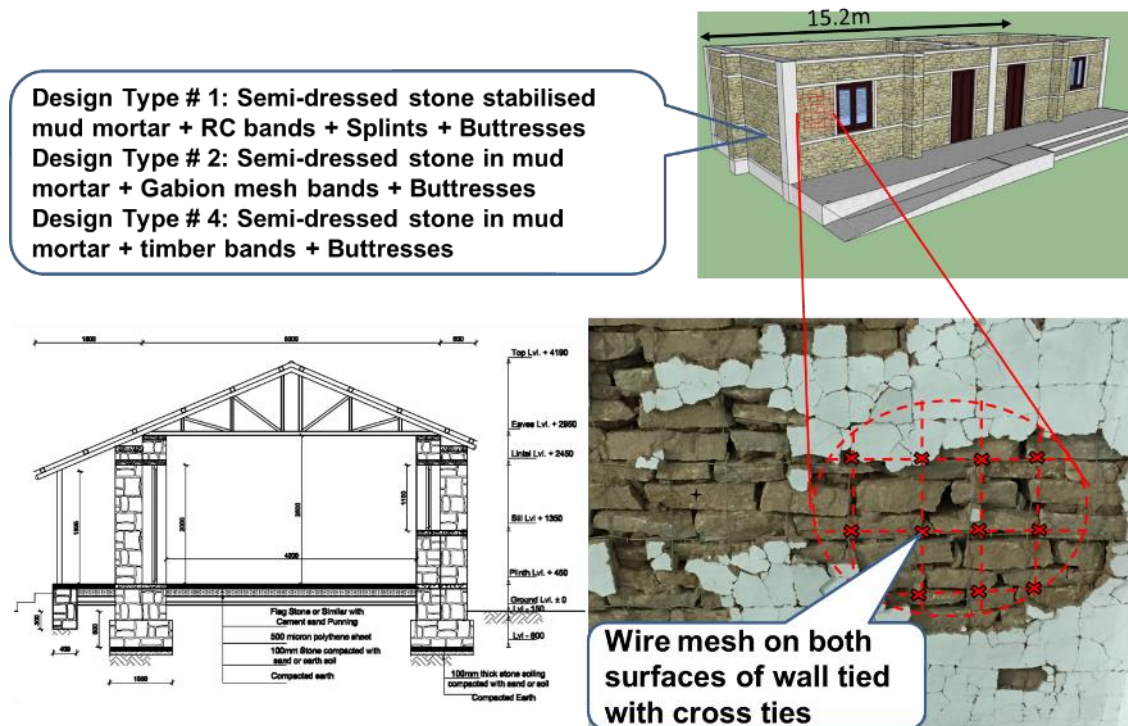


Figure 2: Prototype details of the proposed building (DT 1)

3 DESIGN AND CONSTRUCTION OF THE MODEL BUILDINGS

In order to confirm compliance of the proposed Type Designs for the school buildings to the relevant seismic Standards, dynamic shake table tests were performed on three 1/3rd scale and another three 2/3rd scale semi-dressed stone masonry model buildings. The shake table tests of the 1/3rd and 2/3rd scale models were a compromise, as initially the goal was to test at least 1/2 scale models to minimise scaling effect and difficulty in scaling of stones and mortar layers (Bothara, Ingham, & Dizhur, 2018). The model buildings were provided with the earthquake resistant elements such as sill, lintel and eaves bands including surface containment mesh as discussed earlier. No additional weight or mass was added to the model buildings for stress similitude to avoid change in boundary conditions and to avoid turning a distributed mass system into a lumped mass system. The additional mass would have required a strong ceiling, which would have acted as a rigid diaphragm. All 2/3rd scale models were built on the table, whereas the 1/3rd scale models were built off the table on a rigid concrete base slab.

The data obtained during shake table testing is still being processed and only a summary is being reported herein. The shake table test results obtained were converted to prototype response according to the similitude requirements. The response acceleration values were multiplied by 0.33 and 0.67 to obtain the prototype values for 1/3rd and 2/3rd scale models respectively.

3.1 Model Fabrication and Test Specimens

The geometry of the building and its elements (including wire diameters) were linearly scaled down to 1/3rd and 2/3rd sizes of the prototypes. This scaling resulted in a 2.54 m (L)×1.97 m (B)×1.32 m (H) and 5.08 m (L)×3.94 m (B)×2.64 m (H) including roof space for the 1/3rd and 2/3rd reduced scale model buildings

respectively. The stones were scaled down to 1/3rd and 2/3rd scale to suit the scaled model buildings so that the number of bedding planes remained the same as for the prototypes. For improvement in mortar characteristics, cement stabilised mud mortar was used for DT 1, but for the other building models mud mortar was used. Efforts were made to keep the mortar to a minimum thickness. To span window and door openings, reinforced concrete or timber lintels were provided. The roof was constructed using a light metal roof supported by a timber structure. No eaves or roof bracing were provided to stabilise walls under face load.

Attempts were made to simulate the field conditions of the earthquake-affected areas of Nepal while constructing the model buildings and test specimens. To simulate the field conditions, quality control of the construction materials and labourer skills was kept to a minimum, resulting in a large variation in the test results. Two issues were noted during the stone preparations processes: (i) because stone is a natural material, the shapes and sizes and dressability of the stones depends largely on the mineralogy and bedding plane orientation of the stones, which are highly variable even in a short geographical stretch (Figure 3), (ii) the stone masons are habitually used to working with the stones available in the areas of their work, and hence find it difficult to replicate stone masonry from other areas. These two issues made it extremely difficult to accurately replicate stone masonry for testing that was similar to that found in Nepal. All the model buildings were covered with mud plastered and whitewashed, in order to facilitate crack identification during testing. Refer to Figure 4 for photographs of the building models under construction.



(a) Intermixing of double and single thickness stones



(b) Relatively shorter but thicker stones



(c) More clearly defined bedding planes, sharp edges of stones

Figure 3: Variation in semi-dressed stone masonry walls within short stretches in the earthquake-affected areas of Nepal



(a) Model building under construction (DT 1)



(b) Close-up view of stone wall (wire mesh on the wall is stitch) (DT 2)



(c) RC band and splints under construction (DT 1)

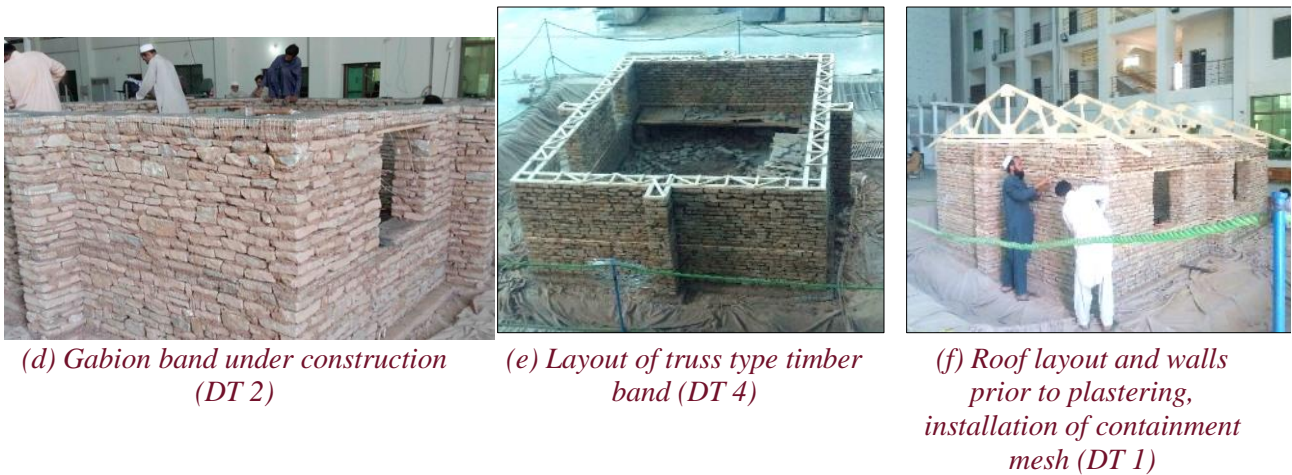


Figure 4: Snapshots of model buildings (2/3rd scale) construction

3.2 Material and subassembly testing

A comprehensive material and subassembly testing programme was designed to characterise construction materials and masonry. The material tests included mortar cube and stone cylinder compression tests, and tensile tests of galvanised wires and reinforcing bars. Subassembly tests included compression tests of masonry prisms, diagonal compression tests of wallettes and in-plane quasi-static cyclic testing of masonry piers (Figure 5). The stone masonry subassemblies were constructed in both stabilised and unstabilised mud mortar with and without surface containment. The non-standard nature of the construction materials and a lack of quality control during construction of the test specimens led to a large variation in the test results of the materials and subassemblies.



Figure 5: Testing of subassemblies

3.3 Experimental Set-up and Loading Protocol

All the model buildings were primarily shaken in the transverse direction considering the high vulnerability of the long walls (refer Figure 6) when subjected to face loading. In addition to transverse shaking, the 1/3rd scale DT 2 model buildings were also tested in the longitudinal direction after shaking these models in the transverse direction after repair. The model buildings were subjected to gradually increasing intensity (i.e. PGA) of shaking up to 1.0g.

Through this loading protocol, the response of the URM buildings to different levels of seismic hazard was inferred, which is in principle similar to the multi-level seismic performance assessment (MSPA) concept (Bradley, Dhakal, Mander, & Li, 2008) except that the rigorous probabilistic earthquake record selection process (Dhakal, Mander, & Mashiko, 2006) was not followed. To track softening of the model buildings, the buildings were subjected to pulse excitations after each episode of significant excitation. After every test run, the model was inspected for possible damages, which were recorded/documentated in the form of visual observations, still photographs and continuous recording through cameras (CCTV and DSLRs).

Accelerometers and linear potentiometers were employed at the eaves and lintel levels and at the base of the buttresses in both out-of-plane and in-plane walls to capture the response of the model buildings during dynamic excitation. Accelerometers were also installed on the shake tables to acquire the response of the shake table to input signals. Potentiometers were employed to measure model displacement with respect to the table platform and the intensity of out-of-plane rocking at the base of the buttress to the wall.



(a) One of the 2/3rd scale model buildings (DT 1)



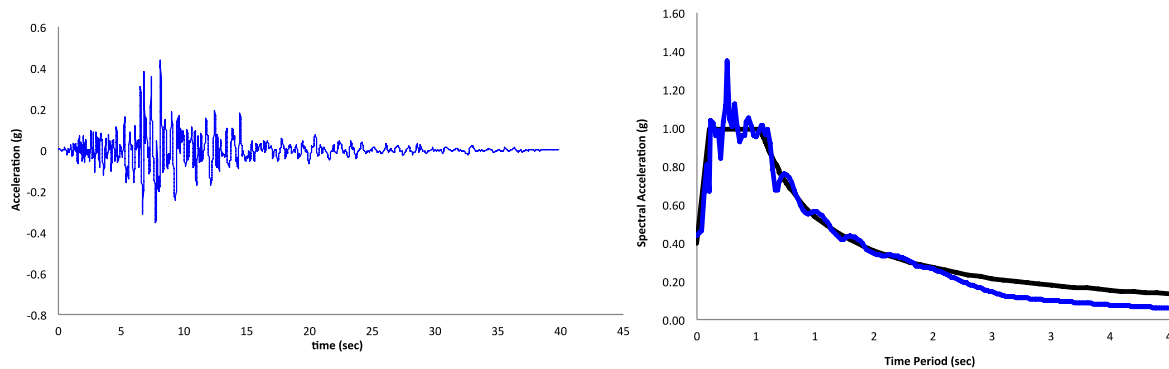
(b) One of the 1/3rd scale model buildings (DT 4)

Figure 6: Testing of the model buildings on the shake table during (testing in transverse direction). Accelerometers were installed inside the red boxes

The 2/3rd scale model buildings were tested on a 60-ton shake table, and were subjected to sinusoidal base excitation of varying frequency and base imposed displacement to produce moderate-to-strong acceleration base excitation, to push the structure from an elastic to an inelastic state in a progressive manner. The input frequencies were varied between 2 Hz and 12 Hz and the base target displacements were selected based on the pseudo-relationship, varying from 1.5 mm to maximum displacement, calculated to not exceed the base acceleration of more than 1.0g, which is the maximum acceleration limit of the seismic simulator. Taking into account different combinations of input frequency and base target displacement, a total of up to 27 runs were carried out. As all the model buildings survived shaking of 1.0g PGA before concluding the shake table tests, the models were subjected to long duration shaking close to a PGA of 1.0g at their resonance frequency to understand degradation of the models. Some variations were made to the test sequence to best-suit the situation, where required.

The 1/3rd scale model buildings were tested on an 8-ton shake table. These models were tested under earthquake acceleration records, which comprised of the base excitations for the transverse shaking, which included: (i) acceleration time history of the Northridge (USA) earthquake of 17 January 1994 record at 090 CDMG STATION 24278 (Main Shaking) (Figure 7a); (ii) KIRT_NS. The KIRT-EW time history was recorded at Kirtipur, Kathmandu on a rock site from the 25 April 2015 Gorkha earthquake and was used as a supplementary test. To meet the objective requirement of verification of compliance of the proposed design to the applicable seismic Standards, the acceleration time history was matched to the code specified design acceleration spectrum of the Indian Seismic Standard (IS, 1993) (refer Figure 7b). To meet the scaling requirements, the

acceleration time history frequency was increased by a Scale factor^{0.5} = $3^{0.5} = 1.73$ in the present case. Shaking of the shale table was progressively increased from 5% to 240% to understand the behaviour of the model under design level forces and extreme level forces that may be expected in very rare earthquakes. Tests were also conducted on 1/3rd scale model buildings after removing 50% of the containment mesh of one of the in-plane walls and 100% of the containment mesh of another in-plane wall to gauge the sensitivity of the containment mesh to the seismic resiliency of the building. Some variation in shaking sequence were made as required. After completion of main tests, the models were subjected to artificially elongated long duration shaking to understand degradation of the models.



(a) Matched time history of Northridge (USA) earthquake of 17 January 1994 recorded at Station : 090 CDMG STATION 24278
The Northridge (USA) earthquake of January 17, 1994.

(b) Matching of acceleration record spectrum and code specified design spectrum (the design spectra includes Importance factor = 1.5 and Load factor = 1.5)

Figure 7: Main shaking time history and spectra matching

4 TEST OBSERVATIONS AND RESULTS

4.1 Visual observation

Under low to moderate shaking, the model buildings did not show any significant/visible damage in structural or non-structural components, but when subjected to moderate to strong shaking ($\approx 0.6g$), horizontal cracks were observed for all of the tested model buildings. All the model buildings survived input peak ground acceleration of 1.0 g without triggering any unstable modes of failure. Even the long duration intense shaking could not make the building or its components unstable. The failure mechanism of the in-plane walls was mostly dominated by rocking and sliding along many horizontal bedding planes. The behaviour of the face-loaded walls was primarily dominated by out-of-plane flexural bending. At high-intensity shaking, the buttresses and face-loaded walls rocked globally. It is likely that the sliding and rocking of in-plane and out-of-plane loaded walls limited seismic demand on the model buildings, which helped the survival of the tested buildings.

Interestingly, damage patterns and performance of the 1/3rd and 2/3rd scale model buildings with the same seismic resistance elements were in very good agreement. Similarly, the observed seismic performance of model buildings with different earthquake resistance features were also generally similar. However, there were differences regarding how the model building behaved with different earthquake resilient features. A few examples are: the in-plane walls of the model buildings with RC bands suffered more damage compared to the in-plane walls of the model buildings with timber and gabion bands, indicating a global in-plane mechanism of the model under base excitation. In contrast to this, the face-loaded walls of buildings with timber and

gabion bands flexed more violently than did the face loaded walls of the building with RC bands, indicating a dominant out-of-plane mechanism of these building types. This observation indicates that the difference in stiffness of the bands constructed of different materials ensured different levels of building integrity, thus, influencing the hierarchy of damage. In the case of buildings with timber bands, sliding of bands was observed whereas separation of bands and masonry was observed in the case of the model building with RC bands. Neither sliding nor separation was observed between bands and adjoining stones in the buildings with gabion bands, most likely because of the same material properties of the walls and bands tying the walls.

Under extreme shaking, all the model buildings showed significant sliding and rocking of stones in the in-plane wall panels and induced lateral displacement. The containment wires prevented the development of large cracks and dislodging of stone. Further to this, containment wires ensured integrity of walls which allowed re-centering of the building subjected to reverse cycle loading, and the wall panels were observed to be without significant residual permanent deformations. Tremendous energy dissipation capacity has been observed in the model, which was due to well-distributed cracks within all of the walls, as well as horizontal sliding and rocking of stones at multiple locations in the in-plane wall panels.

To investigate sensitivity of stability of the walls to the containment mesh, the 1/3rd scale model buildings of DT 1 and DT 2 were also tested after removing 50% and 100% of the containment mesh from the in-plane walls. Once the containment mesh was fully removed from the in-plane walls, the dislodging and falling of the stones off the wall started, and degradation of the wall was rapid. However, the partial containment mesh was still able to contain the masonry units in the in-plane wall. Figure 8 presents a few of the photographs of models under testing.



(a) Spalling of plaster and sliding of stones, interior face of 2/3rd scale model (DT 1)



(b) Close-up view of wall, note wide cracks due to sliding of stones, exterior face of 2/3rd model (DT 1)



(c) Partial removal of containment mesh, note holes in the wall as result of falling of stones (1/3rd scale, DT 1)



(e) Out-of-plane movement face-loaded wall (DT 4)

(d) Plaster spalling, significant sliding and dislocation of masonry units (2/3rd scale, DT 2)



(f) Breaking of timber band (DT 4)

Figure 8: Photographs of tested model buildings (arrow shows direction of shaking of table)

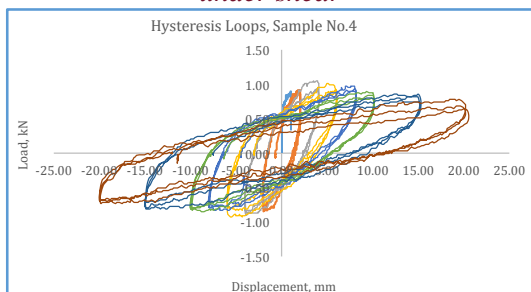
Figure 9 presents force-displacement plots of wall piers with and without surface containment mesh. From the plots, it is obvious that the containment mesh was able to increase force and deformation capacity of the piers, which was also observed with multiple stone sliding planes, resulting in distributed damage over the whole pier. Also, it can be confirmed from the stable and fat hysteretic response of walls that the models with containmnet exhibit significant energy dissipation, which is an essential parameter for controlling seismic demands (forces and defoamtions) and limiting structural damages under earthquake induced lateral vibrations.



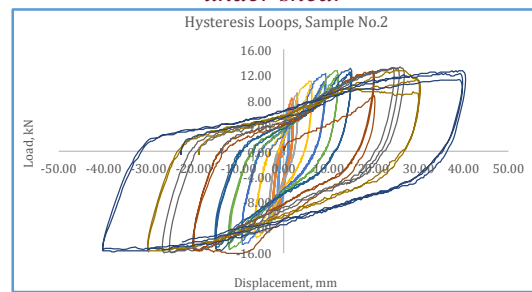
(a) Testing of wall pier without containment mesh under shear



(b) Testing of wall pier with containment mesh under shear



(c) Force-displacement plot of wall pier without containment mesh under in-plane lateral load



(d) Force-displacement plot of wall pier with containment mesh under in-plane lateral load

Figure 9: Force-displacement hysteretic loops of the wall piers buildings (arrow shows direction of push-pull)

4.2 Fundamental periods

Free vibration tests data were analysed for measurement of fundamental frequency of models. The uncracked fundamental period of model was measured using the data from free vibration test runs. The time history response of acceleration recorded at the eave level was obtained and analysed in SeismoSignal for base line correction and filtering. Fourier amplitude of acceleration was correlated with the frequency to obtain the power spectral density (PSD). Figure 10 presents the PSD obtained for 2/3rd model for out-of-plane responding wall for TD 2. It is interesting to note that the fundamental period of the in-plane and out-of-plane walls were very different in the case of the models with timber and gabion, whereas the same was very close with the RC bands. To understand the behaviour, the data is being further analysed.

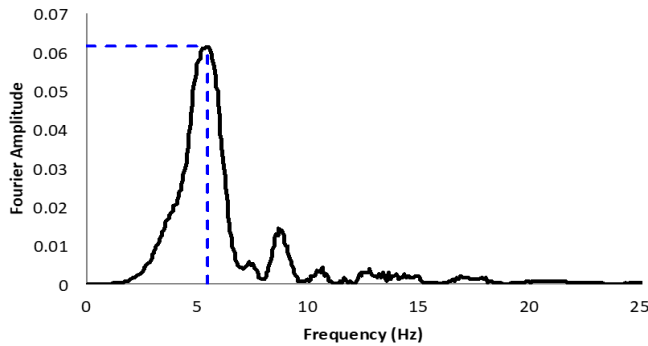


Figure 10: PSD developed for free vibration acceleration response of 2/3rd model for out-of-plane response

4.3 Damping

The decay function for the time history of the response acceleration as proposed by Chopra (2003) was used to calculate the model damping:

$$\zeta = \frac{1}{2n\rho} \ln\left(\frac{A_1}{A_n}\right)$$

where ζ represents elastic damping coefficient; A_1 represents the peak amplitude of response displacement at reference point 1; A_n represents the peak amplitude of response displacement at reference point after n cycles; and n represents the number of cycles between the peaks.

The model damping was calculated from the free vibration tests of the model, carried out by means of table impulse loading. The structure displacement response at the top was considered and analysed for calculating the decay in the displacement history. The damping was calculated from the logarithmic decay of the last two cycles. The structural damping was found to be between 20 and 30% for the different building models.

4.4 Ductility and Response Modification factor

In the present research the seismic response modification factor R of structural models is calculated by the procedure used by Ali et al (2013). Generally, R factor for a structure can be calculated knowing the inelastic lateral force-deformation behaviour of the structure.

$$R = \frac{V_e}{V_s} = \frac{V_e}{V_y} \cdot \frac{V_y}{V_s} = R_m \cdot R_s$$

Where, V_e represents the elastic force the structure will experience, if responded elastically under earthquake demand; V_y represents the idealized yield strength of the structure; V_s represents the design base shear force; R_m represents the ‘ductility factor’, ie structure ductility dependent factor, R_s represents the ‘overstrength factor’, i.e. structure overstrength dependent factor. The overstrength factor R_s is calculated directly from the lateral force-deformation capacity curve of the structure (i.e. dividing the idealized yield strength over the

structure design strength), however, the ductility factor R_{μ} is related to the structural ductility (Newmark and Hall, 1982, Tomazevic, 1999) as given:

Short Period	$T < 0.20 \text{ sec.}$	$R_m = 1.0$	Structure Vibration Period: $T = 2\rho \sqrt{\frac{m}{k_y}}$
Intermediate Period	$0.2 \text{ sec.} < T < 0.5 \text{ sec.}$	$R_m = \sqrt{2m - 1}$	
Long Period	$T > 0.5 \text{ sec.}$	$R_m = m$	

where T is the pre-yield vibration period of idealized single degree of freedom system. The R -factor was found in the range of 2.5 for in-plane and out-of-plane walls.

5 CONCLUSIONS

The paper has presented a number of school building designs that utilise abundantly available local semi-dressed stone and mud as construction materials combined with the use of limited imported materials such as cement, reinforcing bars and steel wires to enhance the earthquake resilience for the remote areas of Nepal. To verify compliance of these proposed designs to applicable seismic standards, three 1/3rd scale and another three 2/3rd scale one-storey model buildings were tested on shake tables up to 1.0 g PGA. All the models survived the applied shaking without suffering any unstable mode of failures. It was also observed that even during severe rocking and sliding of the masonry along multiple bedding planes, the containment mesh was able to hold the masonry together and helped self-centering of the building structures. The sensitivity tests conducted by partial and full removal of the containment mesh reinforced this observation. The stones sliding over multiple paths enabled the structure to dissipate input energy, and thereby, control seismic demands. The same is also confirmed through in-plane quasi-static cyclic tests on masonry piers. The extensive experimental investigation has illustrated that it is feasible to make stone masonry school buildings constructed using stone masonry in mud mortar earthquake resilient

The technology developed herein has the potential to be modified and adopted for residential buildings and seismic retrofitting of existing stone masonry buildings in Nepal and in other seismically active countries around the world, particularly in the developing countries.

The results obtained from the experimental testing needs to be generalised for other shape and size of stone masonry buildings. The investigation now needs to be extended to two storeys plus attic buildings which are commonly found in hills and mountains of Nepal.

6 ACKNOWLEDGEMENTS

The experimental testing work presented here was completed under the Asian Development Bank's (ADB) financial and technical assistance to the Government of Nepal under Earthquake Emergency Assistance Project after the 2015 Gorkha earthquake. The granting of permission from the Central Level Project Implementation Unit (Education), Government of Nepal's wing responsible for construction of school buildings (the recipient of the ADB's grant), to use the research findings is thankfully acknowledged. All the experimental testing work presented here are being completed at the Earthquake Engineering Center of University of Engineering and Technology (UET), Peshawar, Pakistan under a contract between the ADB and the UET. Efforts of the UET research team is thankfully acknowledged.

7 REFERENCES

Arya, A.S., Boen, T. & Ishiyama, Y. 2013. *Guidelines for Earthquake Resistant Non-Engineered Construction*. Paris: United Nations Educational, Scientific and Cultural Organization. doi:ISBN 978-92-3-000032-5

- Bothara, J.B. & Hıçyılmaz, M.O. 2008. General Observations of Building Behaviour During the 8th October 2005 Pakistan Earthquake, *Bulletin of the New Zealand Society for Earthquake Engineering*, Vol 41(4) 209-233.
- Bothara, J.K., Dhakal, R.P., Dizhur, D. & Ingham, J.M. 2016. The Challenges of Housing Reconstruction after the April 2015 Gorkha, Nepal Earthquake, *Technical Journal of Nepal Engineers' Association, Special Issue on Gorkha Earthquake 2015*, XLIII-EC, Vol 30(1) 121-134.
- Bothara, J.K., Ingham, J. & Dizhur, D. 2018. Understanding, Experience and Research on Seismic Safety of Low-Strength Loadbearing Masonry Buildings, *16th Symposium on Earthquake Engineering, Paper No.: Kn2*, 1-26. Roorkee, India.
- Bradley, B.A., Dhakal, R.P., Mander, J.B. & Li, L. 2008. Experimental multi-level seismic performance assessment of 3D RC frame designed for damage avoidance, *Earthquake Engineering and Structural Dynamics*, Vol 37(1) 1-20.
- Chopra, A.K. 2003. *Dynamics of structures: Theory and applications to earthquake engineering*, 3rd Edition, Prentice-Hall, NJ, USA.
- Dhakal, R.P., Mander, J.B. & Mashiko, N. 2006. Identification of critical ground motions for seismic performance assessment, *Earthquake Engineering and Structural Dynamics*, Vol 35(8) 989-1008.
- Dizhur, D., Dhakal, R.P., Bothara, J.K. & Ingham, J.M. 2015. Building Typologies and Failure Modes Observed in the 2015 Gorkha (Nepal) Earthquake, *Bulltin of New Zealand Society for Earthquake Engineering*, Vol 49(2) 211-232.
- Gautam, G. & Chaulagain, D. 2016. Structural Performance and Associated Lessons to be Learned from World Earthquakes in Nepal after 25 April 2015 (MW 7.8) Gorkha Earthquake, *Engineering Failure Analysis*, Vol 68 222-243.
- IS. 1993. *IS13828-1993 Improving Earthquake Resistance of Low Strength Masonry Buildings - Guidelines*. 9 Bahadur Shah Zafar Marg New Delhi 110002: Bureau of Indian Standards Manak Bhavan.
- Jagadish, K.S., Raghunath, S. & Rao, K.N. 2002. Shake Table Studies on Masonry Building Model with Containment Reinforcement, *Journal of Structural Engineering*, Vol 29(1) 9-17.
- Navaratnarajah, S., Mayorca, P. & Meguro, K. 2012. Shake Table Tests on One-Quarter Scale Models of Masonry Houses Retrofitted with PP-Band Mesh, *Earthquake Spectra*, Vol 28(1) 277-299. doi:10.1193/1.3675357
- Navaratnarajah, S., Sakurai, K. & Meguro, K. 2009. Experimental Study of PP-Band Retrofitted Masonry Structure made of Shapeless Stone. *SEISAN-KENKYU*, 61(6), 1051-1054. Retrieved September 12, 2018, from https://www.jstage.jst.go.jp/article/seisankenkyu/61/6/61_6_1051/_pdf
- NBC. 1994. *NBC203-1994: Guidelines For Earthquake Resistant Building Construction: Low Strength Masonry*. Kathamandu: Nepal National Building Code, Department of Urban Development and Building Construction, Ministry of Physical Planning and Works, Government of Nepal.
- Newmark, N.M. & Hall, W.J. 1982. *Earthquake spectra and design*, Earthquake Engineering Research Institute, Oakland, CA.
- NNBC. 1994. *NBC204-1994: Guidelines For Earthquake Resistant Building Construction: Low Strength Masonry*. Kathamandu: Nepal National Building Code, Department of Urban Development and Building Construction, Ministry of Physical Planning and Works, Government of Nepal.
- NRA. 2016. *Nepal Earthquake 2015: Post Disaster Recovery Framework 2016-2020*. Kathmandu, Nepal: National Planning Commission, Government of Nepal.
- Tomazevic, M. & Velechovsky, T. 1992. Some Aspects of Testing Small-scale Masonry Building Models on Simple Earthquake Simulators, *Earthquake Engineering and Structural Dynamics*, Vol 21 945-963.
- Tomazevic, M. 1999. *Earthquake Resistant Design of Masonry Buildings*, Imperial College Press, London, UK.